RSC Advances

ROYAL SOCIETY OF CHEMISTRY

www.rsc.org/advances

Cite this: DOI: 10.1039/c0xx00000x

www.rsc.org/xxxxxx

ARTICLE TYPE

Properties and Photocatalytic Performance of Polypyrrole and Polythiophene Modified g-C_3N_4 Nanocomposites

Shaozheng Hu [a], Lin Ma [a], Haoying Wang [a], Lei Zhang [a], Yanfeng Zhao [a] and Guang Wu [b,*]

Received (in XXX, XXX) Xth XXXXXXXXX 20XX, Accepted Xth XXXXXXXXX 20XX

DOI: 10.1039/b000000x

Polypyrrole (Ppy) and polythiophene (Ptp) modified g-C_3N_4 nanocomposites were prepared using simple sonochemical approach and their photocatalytic performances are compared. XRD, N_2 adsorption-desorption, FTIR, UV-Vis, SEM, EIS, XPS and PL are used to characterize the prepared composite materials. The results reveal that no obvious difference is observed in grain size, crystal phase and structural properties between two series of polymer modified g-C_3N_4 nanocomposites. The polymer modification can decrease the band gap which is beneficial for the visible-light absorption. The introduction of polymers does not act as visible light sensitizer but facilitates the separation and transport of photogenerated carriers. The visible-light-driven Rhodamine B (RhB) photodegradation performance was carried out to test the catalytic activity of as-prepared g-C_3N_4 based nanocomposites. Compare with Ppy, stronger interaction exists between Ptp and g-C_3N_4 which cause the higher electron-hole separation rate, thus shows a better photocatalytic activity and stability.

Introduction

Toxic organic pollutants have become one of the main sources of water pollution. All those pollutants discharged from factories are harmful to the environment and human health. More severely, they are difficult to remove by traditional treatment methods because of the high stability.[1] Most of the azo dyes and fluorine dyes, such as aromatic amines, are suspected to have carcinogenic effects, so the international environmental standards are becoming more and more stringent. Correspondingly, the treatment of organic pollutants discharged into the environment has also been developed.[2] In recent years, it has been proved that the photocatalytic oxidation technology is an effective method for the environment remediation. Titanium dioxide, as a common photocatalyst, has been widely studied for pollutant degradation and other applications. However, it can only be excited by ultraviolet light irradiation because of its large band gap (3.0~3.2 eV).

In 2009, Wang et al. first reported a metal-free graphite-like carbon nitride (g-C_3N_4) exhibiting photocatalytic activity for H_2 production under visible light.[3] It has been shown that g-C_3N_4 has a suitable band gap energy of approximately 2.7 eV. Besides, g-C_3N_4 possesses good chemical and thermal stability as well as fascinating electronic properties, thus has attracted intensive interest for its promising applications in splitting water to produce H_2, decomposition of organic pollutants and organic synthesis under visible light. However, the photocatalytic activity of pure g-C_3N_4 is poor due to its low light-absorbance and fast recombination of photogenerated electron-hole pairs. To overcome those problems and improve the photocatalytic activity, various methods have been developed, such as metal and nonmetal doping, protonating by strong acids, preparation of porous g-C_3N_4 and designing heterojunction composite.[4-9]

Materials like polymer species with conjugated π electronic structures and visible-light absorption are nontoxic and can be good candidates for the fast separation of photogenerated charge carriers.[10] Yan et al.[11] introduced poly(3-hexylthiophene) (P3HT) to form a P3HT-g-C_3N_4 heterojunction and reported that the H_2 evolution rate was increased 300 times from water with Na_2S and Na_2SO_3 as electron donors under visible light irradiation. Ge et al.[12] synthesized polyaniline-graphitic carbon nitride (PANI-g-C_3N_4) composite by "in situ" deposition oxidative polymerization of aniline monomer in the presence of g-C_3N_4 powder. The PANI-g-C_3N_4 composites show enhanced performance for MB photodegradation under visible-light illumination. He et al.[13] prepared graphitized polyacrylonitrile (g-PAN) modified g-C_3N_4 nanosheets through a facile one-step thermal condensation of PAN and melamine. The 5.0 wt.% g-PAN/g-C_3N_4 composite exhibited optimal H_2 evolution rate of 37 $\mu mol \cdot h^{-1}$ under visible light, exceeding 3.8 times over pristine g-C_3N_4. Though the introduction of P3HT, PANI and g-PAN is effective to improve the photocatalytic performance, it is expensive and difficult to obtain through organic synthesis which inhibits their practical application. Ppy and Ptp are typical conductive polymers with high conductivity, stability in the oxidized state and interesting redox properties. Moreover, PPy and Ptp nanoparticles are cheaper and easier to be synthesized than that of P3HT, PANI and g-PAN. Introducing dispersively distributed Ppy or Ptp nanoparticles on g-C_3N_4 sheets can form the surface junctions to increase the separation rate of photogenerated charge carriers. In this work, Ppy and Ptp modified g-C_3N_4 nanocomposites were prepared separately. The properties and photocatalytic

performance of as-prepared Ppy and Ptp modified g-C_3N_4 nanocomposites were compared.

Experimental

Preparation and characterization

3 g melamine was annealed at 520 °C for 2 h at a rate of 5 °C·min^{-1}. Then the g-C_3N_4 was obtained. The yield of g-C_3N_4 was approximately 50%. Ppy and Ptp were prepared according to previous reports.[14,15] The polymer/g-C_3N_4 composite photocatalyst was fabricated via a sonochemical approach. 0.1 g g-C_3N_4 was dispersed in 100 mL deionized water to obtain a suspension. Then, 0.0015~0.004 g of Ppy or 0.0005~0.0025 g of Ptp was added into above suspension. The suspension was treated with ultrasonication for 12 h. The polymer/g-C_3N_4 composite was obtained by filtering the suspension and drying at 80 °C for 12 h. The polypyrrole/g-C_3N_4 and polythiophene/g-C_3N_4 composites were denoted as Ppy(x%)-CN and Ptp(x%)-CN, where x% stands for the weight percentage of polymer to g-C_3N_4.

XRD patterns of the prepared samples were recorded on a Rigaku D/max-2400 instrument using Cu-Kα radiation (λ = 0.15418 nm). The scan rate, step size, voltage, current, and scanning range was 0.05 °/min, 0.01 °, 40 kV, 30 mA, and 10~40 °. Scanning electron microscope (SEM) images were collected using a field emission scanning electron microscope (S-4200, Hitachi, Tokyo, Japan) with an accelerating voltage of 15 kV. Elemental analysis was performed with a vario EL cube from Elementar Analysensysteme GmbH. UV-Vis diffused reflectance spectroscopy measurement was carried out on a JASCO V-550 model UV-Vis spectrophotometer, using $BaSO_4$ as the reference ("white" standard) Nitrogen adsorption was measured at -196 °C on a Micromeritics 2010 analyzer. BET surface area (S_{BET}) was calculated according to the adsorption isotherm. FTIR spectra were recorded on Nicolet 6700 IR spectrometer by using KBr pellets. All the samples were activated at 393 K before the measurement. BET Surface area (S_{BET}) was calculated according to the adsorption isotherm. PL spectra were measured at room temperature with a fluorospectrophotometer (FP-6300) using a Xe lamp as excitation source. XPS measurements were conducted on a Thermo Escalab 250 XPS system with Al Kα radiation as the exciting source. The binding energies were calibrated by referencing the C 1s peak (284.6 eV) to reduce the sample charge effect. Electrochemical impedance spectra (EIS) made from these as-made materials were measured via an EIS spectrometer (EC-Lab SP-150, BioLogic Science Instruments) in a three-electrode cell by applying 10 mV alternative signal versus the reference electrode (SCE) over the frequency range of 1 MHz to 100 mHz. The cyclic voltammograms were measured in 0.1 M KCl solution containing 2.5 mM $K_3[Fe(CN)_6]/K_4[Fe(CN)_6]$ (1:1) as a redox probe with the scanning rate of 20 mV·s^{-1} in the same three electrode cell as EIS measurement.

Photocatalytic Reaction

RhB was selected as the model compound to evaluate the photocatalytic performance of the prepared g-C_3N_4 based catalysts in an aqueous solution under visible light irradiation. In 200 mL aqueous solution of Rhodamine B (RhB) (10 mg·L^{-1}), 0.05 g catalyst was dispersed and the solution was left in an ultrasound generator for 10 min. The suspension was transferred into a self-designed glass reactor, stirred for 30 min in darkness to achieve the adsorption equilibrium. In the photo-reaction , the suspension was exposed to a 250 W high-pressure sodium lamp with main emission in the range of 400-800 nm and air was bubbled at 130 mL·min^{-1} through the solution. The UV light portion of sodium lamp was filtered by 0.5 mol·L^{-1} $NaNO_2$ solution.[16] All runs were conducted at ambient pressure and 30 °C. At given time intervals, 4 mL suspension was taken and immediately centrifuged to separate the liquid phase from the solid catalyst. The concentrations of RhB before and after reaction were measured by UV-Vis spectrophotometer at wavelength of 550 nm.

Results and discussion

Fig. 1 shows the photocatalytic activities of prepared nanocomposite catalysts under visible light. Control experiment result indicates that the RhB degradation performance can be ignored in the absence of either irradiation or photocatalyst, indicating that RhB is degraded via photocatalytic process. The absorption ability of g-C_3N_4 does not improve after polymer modification. Unsurprisingly, neat g-C_3N_4 exhibits low degradation rate (33%) because of the high electron-hole recombination rate. For Ppy(x%)-CN and Ptp(x%)-CN, RhB degradation rate improves obviously. Ppy(2.5%)-CN and Ptp(1.5%)-CN exhibit the highest degradation rates in two series of polymer modified g-C_3N_4 catalysts (74% and 92%). The Ptp(x%)-CN series catalysts show much higher activity than that of Ppy(x%)-CN. Furthermore, the absorbance of the RhB solutions over g-C_3N_4, Ppy(2.5%)-CN and Ptp(1.5%)-CN in the photocatalytic reaction are investigated (Fig. 2). It is shown that the maximum absorption peaks of the RhB solutions at ~554 nm do not shift and no new absorption peak is observed. The vanishing absorptions of the ultraviolet region at 250-380 nm proves that the benzene/heterocyclic rings of the RhB molecule may be destroyed.[17]

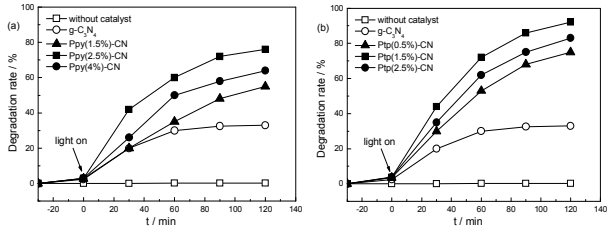

Fig. 1 Photocatalytic performances of as-prepared g-C_3N_4, Ppy(x%)-CN (a) and Ptp(x%)-CN (b) in the degradation of RhB under visible light irradiation.

The XRD patterns of g-C_3N_4, Ppy(x%)-CN and Ptp(x%)-CN are presented in Fig. 3. Two peaks located at 13.1 ° and 27.2 ° are present for g-C_3N_4. The peak at 13.1 ° corresponds to in-plane structural packing motif of tri-s-triazine units, which is indexed as the (100) peak. The d value is 0.675 nm. The peak at 27.2 ° corresponds to interlayer stacking of aromatic segments with a distance of 0.328 nm, which is indexed as the (002) peak of the stacked conjugated aromatic system. The XRD peak positions and shapes of Ppy(x%)-CN and Ptp(x%)-CN show no change

compared with those of g-C_3N_4, which indicates that the loading of Ppy and Ptp do not influence the crystal structure of g-C_3N_4. The grain sizes of the as-prepared nanocomposites are calculated by their XRD patterns according to the Debye-Scherrer equation.[18] The result shows that no obvious difference in grain sizes is observed (Table 1).

Table 1 Grain sizes, S_{BET}, Pore volume and RhB degradation rate of as-prepared g-C_3N_4, Ppy(x%)-CN and Ptp(x%)-CN

Sample	Grain size (nm)	S_{BET} ($m^2 \cdot g^{-1}$)	Pore volume ($cm^3 \cdot g^{-1}$)	D (%)
g-C_3N_4	48	10	0.07	33
Ppy(1.5%)-CN	46	11	0.08	55
Ppy(2.5%)-CN	45	11	0.08	76
Ppy(4%)-CN	47	10	0.09	64
Ptp(0.5%)-CN	48	11	0.07	75
Ptp(1.5%)-CN	49	11	0.08	92
Ptp(2.5%)-CN	47	10	0.08	83

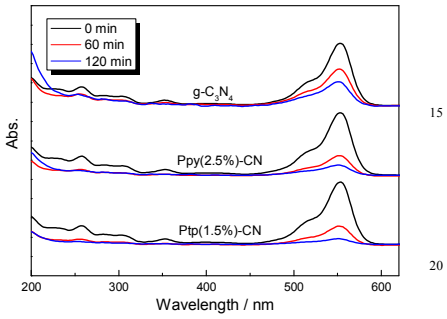

Fig. 2 Absorbance of RhB solutions over g-C_3N_4, Ppy(2.5%)-CN and Ptp(1.5%)-CN.

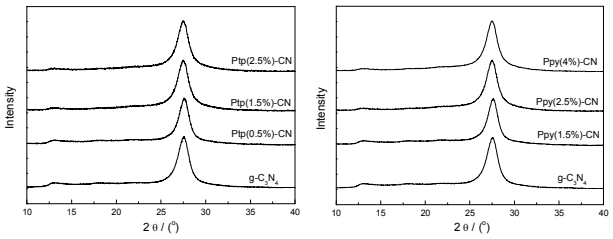

Fig. 3 XRD patterns of as-prepared g-C_3N_4, Ppy(x%)-CN and Ptp(x%)-CN.

Generally, the ability of adsorption, desorption and diffusion of reactants and products are mainly determined by the S_{BET} and pore volume of the catalyst.[19] Therefore, a catalyst with high specific surface area (S_{BET}) and big pore volume is significant to the enhancement of catalytic performance. Nitrogen adsorption and desorption isotherms are measured to characterize the specific surface area of as-prepared g-C_3N_4 based catalysts (Fig. 4). All the catalysts show a type IV isotherm with H3 hysteresis loop, suggesting the presence of mesopores. The hysteresis loop in the low pressure range ($0.4<P/P_0<0.9$) is associated with the intra-aggregated pores. The high-pressure hysteresis loop ($0.9<P/P_0<1$) is related to the larger pores formed between secondary particles. The S_{BET} and pore volume of neat g-C_3N_4 are 10 m^2g^{-1} and 0.07 cm^3g^{-1}, which are very close to that of polymer modified g-C_3N_4 catalysts (Table 1). This is reasonable because, with such a small polymer amount, the surface area and porosity are mainly dominated by g-C_3N_4 ingredient. Based on above results, it is concluded that polymer modification does not change the crystal phase, grain size and structural properties of g-C_3N_4 catalyst.

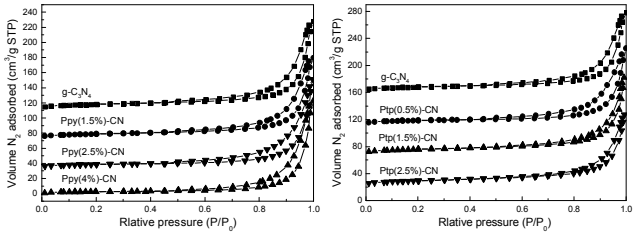

Fig. 4 N_2 adsorption-desorption isotherms of prepared catalysts.

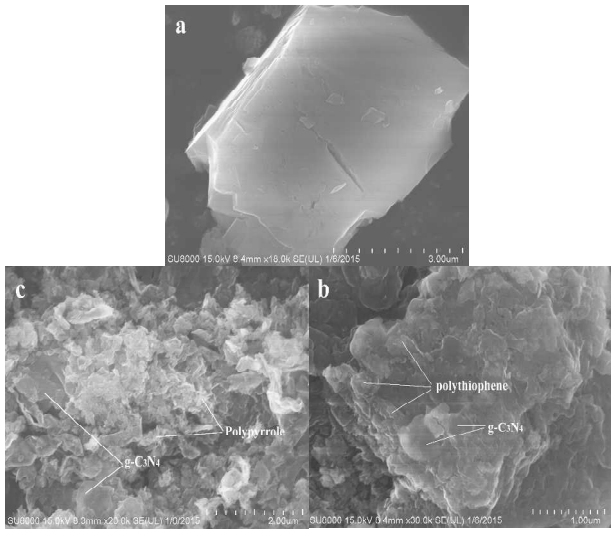

Fig. 5 SEM images of prepared g-C_3N_4 (a), Ptp(1.5%)-CN (b) and Ppy(2.5%)-CN (c).

The morphologies of the representative samples are examined by using SEM analysis (Fig. 5). Fig. 5a indicates as-prepared g-C_3N_4 exhibits smooth layer structure that is similar to the analogue graphite. The size of g-C_3N_4 is 3~4 μm. For Ptp(1.5%)-CN and Ppy(2.5%)-CN (Fig. 5b, c), it can be seen that some polymer little particles attach on the g-C_3N_4 surface. Those particle sizes are 100~200 nm, which is much smaller than that of g-C_3N_4. Therefore, we deduce those particles should be the polymers. Besides, those polymer particles disperse evenly on the

g-C_3N_4 surface. No obvious agglomeration is observed. Such a large contact area between g-C_3N_4 and polymers are favorable for the formation of heterojunction, which facilitates interfacial charge transfer and inhibits electron-hole recombination.

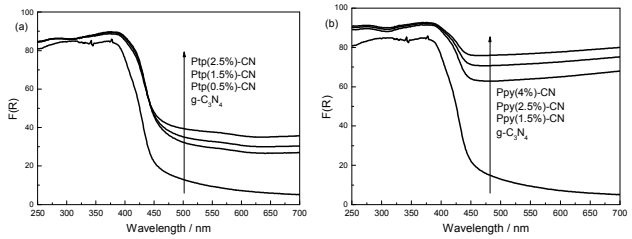

Fig. 6 UV-Vis diffuse reflectance spectra of as-prepared g-C_3N_4, Ppy(x%)-CN and Ptp(x%)-CN.

The UV-Vis diffuse reflectance spectra for the as-prepared g-C_3N_4, Ppy(x%)-CN and Ptp(x%)-CN catalysts are shown in Fig. 6. Obviously, Ppy(x%)-CN and Ptp(x%)-CN catalysts show stronger background absorption due to the black color of Ppy and Ptp. The absorption edge is estimated by the intersection point of the tangent of the curves and the abscissa. For g-C_3N_4, the absorption edge is 477 nm. Ptp (x%)-CN catalysts exhibit the same absorption edge, 496 nm. In the case of Ppy (x%)-CN, the absorption edges show the obvious red shifts with increasing the Ppy concentration. The absorption edges are 539, 563 and 590 nm for Ppy (1.5%)-CN, Ppy (2.5%)-CN and Ppy (4%)-CN respectively. The band gaps are calculated according to the method of Oregan and Gratzel.[20] The band gap energy of g-C_3N_4 is about 2.6 eV, which is in good agreement with the value reported.[21] This value decreases to 2.5 eV for Ptp(x%)-CN series catalysts and to 2.3, 2.2 and 2.1 eV for Ppy(1.5%)-CN, Ppy(2.5%)-CN and Ppy(4%)-CN. It is reasonable that the surface modification of PPy or PTP can not change the band gap of g-C_3N_4. Therefore, this result seems interesting. Dong et al. prepared g-C_3N_4/g-C_3N_4 heterojunction catalyst using urea and thiourea as raw material.[22] The absorption edge and band gap of g-C_3N_4/g-C_3N_4 heterojunction catalyst were located between two components. According to this phenomenon, they confirmed the electronic coupling of these two components in the g-C_3N_4/g-C_3N_4 heterojunction. This result indicates that, when the heterojunction is formed between two components, the absorption edge and band gap of obtained composite catalyst could be changed and different from each component. In this system, the formation of heterojunction between g-C_3N_4 and polymer could change the band absorption and band gap of g-C_3N_4/polymer composite catalyst, leading to this band gap decrease.

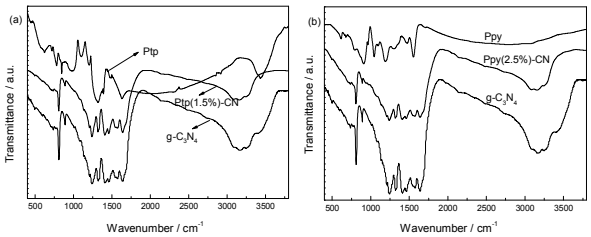

Fig. 7 FTIR spectra of as-prepared g-C_3N_4, Ppy(x%)-CN and Ptp(x%)-CN.

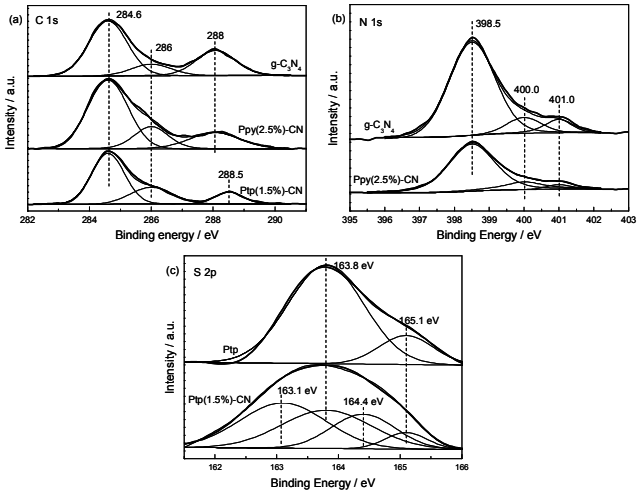

Fig. 8 XP spectra of prepared materials in the region of C 1s (a), N 1s (b) and S 2p (c).

FTIR spectra of as-prepared g-C_3N_4, Ppy(x%)-CN, and Ptp(x%)-CN are shown in Fig. 7. In Fig. 7a, the peaks around 1110 and 1485 cm^{-1} are attributed to the symmetric stretching vibration of C-C and C=C bonds of thiophene. The peak at 780 cm^{-1} is assigned to the bending vibration of C-H bond. Besides, the peak located at ca. 1636 cm^{-1} is attributed to the carbonyl functional group, indicating thiophene is oxidized to some extent.[14] In Fig. 7b, the peaks around 1553 and 1470 cm^{-1} are originated from the stretching vibration of pyrrole.[15] The peaks at 1046 and 1180 cm^{-1} are attributed to the stretching vibration of C-N bond. For g-C_3N_4, a series of peaks in the range from 1200 to 1600 cm^{-1} are attributed to the typical stretching modes of CN heterocycles, while the sharp peak at 810 cm^{-1} is assigned to the bending vibration of heptazine rings, indicating that the synthesized g-C_3N_4 is composed of heptazine units. The broad absorption band around 3200 cm^{-1} is originated from the stretching vibration of N-H bond, associated with uncondensed aminogroups.[23] For Ppy(2.5%)-CN and Ptp(1.5%)-CN, all the characteristic vibrational peaks of g-C_3N_4 are observed, suggesting that the structure of g-C_3N_4 is not changed after polymer modification. No characteristic peak of Ppy (Ptp) in Ppy(2.5%)-CN (Ptp(1.5%)-CN) appears in the spectrum, probably because of the low quantity in the composites.

Fig. 8 shows the XP spectra of prepared materials in the region

of C 1s (a), N 1s (b) and S 2p (c). In Fig. 8a, the binding energy of three samples located at 284.6 eV is attributed to the C-C bond. The binding energy located at 286 eV is attributed to the C-N bond for g-C_3N_4 and Ppy(2.5%)-CN and to the C-S bond of thiophene for Ptp(1.5%)-CN.[24-26] The binding energy at 288 eV for Ppy(2.5%)-CN and g-C_3N_4 should be assigned to C=N bond.[24,25] For Ptp(1.5%)-CN, the binding energy located at 288.5 eV is attributed to the C=O bond,[27] which is consistent with the FTIR result. In Fig. 8b, three components located at 398.5, 400.0 and 401.0 eV for g-C_3N_4 and Ppy(2.5%)-CN were attributed to the sp^2 hybridized aromatic nitrogen atoms bonded to carbon atoms (C-N=C), tertiary nitrogen N-$(C)_3$ groups linking structural motif or amino groups carrying hydrogen ($(C)_2$-N-H) in connection with structural defects and incomplete condensation, and nitrogen atoms bonded three carbon atoms in the aromatic cycles.[25] No obvious difference between them is shown. In Fig. 8c, the binding energy of Ptp located at 163.8 (S $2p_{3/2}$) and 165.1 eV(S $2p_{1/2}$) are attributed to sulfur in thiophene.[27] For Ptp(1.5%)-CN, besides those two peaks, two binding energies located at 163.1 and 164.4 eV are observed. These peaks should be due to the change of chemical environment of sulfur element in thiophene. Partial electrons of electron-rich g-C_3N_4 are transferred to Ptp, leading to the increased electron density of sulfur, thus the binding energy decreases.

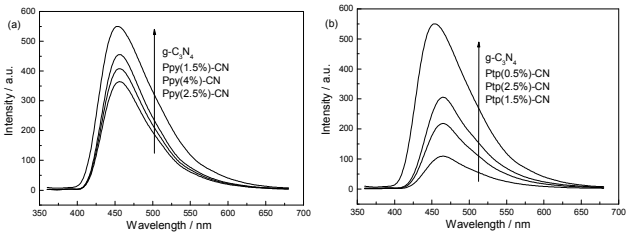

Fig. 9 PL spectra of as-prepared g-C_3N_4, Ppy(x%)-CN (a) and Ptp(x%)-CN (b).

PL is a highly sensitive technique used to provide information on charge separation/recombination of photoinduced charged carriers.[28] In general, the lower PL intensity, the higher separation rates of photogenerated e^-/h^+ pairs, thus the higher photocatalytic activity. Fig. 9 presents a comparison of PL spectra of g-C_3N_4, Ppy(x%)-CN and Ptp(x%)-CN. All the catalysts exhibit similar PL spectra. Ppy(x%)-CN and Ptp(x%)-CN exhibit lower PL intensities compared with g-C_3N_4. This should be due to the interaction between g-C_3N_4 and polymers which cause the charge transfer between them, leading to the lower electron-hole recombination rate. Most of the electrons and holes recombine within a few nanoseconds in the absence of scavengers. If scavenger, such as Ppy or Ptp, is present to trap the electrons or holes, the electron-hole recombination can be suppressed, leading to a photoluminescence quenching. The PL intensities of prepared composites decrease in the order: g-C_3N_4 > Ppy(1.5%)-CN > Ppy(4%)-CN > Ppy(2.5%)-CN; g-C_3N_4 > Ptp(0.5%)-CN > Ptp(2.5%) > Ptp(1.5%), which is opposite to the activity. This result indicates that the difference in activity for polymer modified g-C_3N_4 catalysts is mainly determined by electrons-holes separation efficiency. The stronger interaction between g-C_3N_4 and polymer may cause the better electrons-holes separation efficiency, which results in higher photocatalytic activity. Besides, the PL intensity of Ptp(1.5%) is much lower than that of Ppy(2.5%)-CN, which is probably due to the stronger interaction between electron-rich g-C_3N_4 and Ptp with strong electronegativity oxygen in C=O bond.

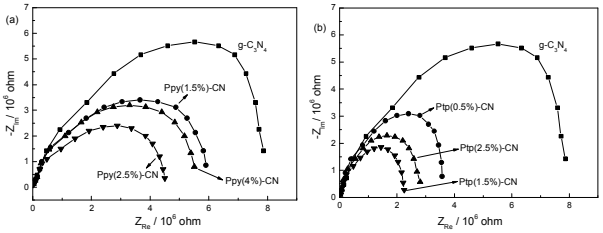

Fig. 10 EIS spectra of as-prepared g-C_3N_4, Ppy(x%)-CN (a) and Ptp(x%)-CN (b).

Electrochemical impedance spectroscopy (EIS) is a very useful tool to characterize the charge-carrier migration, thus was used to further confirm the interfacial charge transfer effect of as-prepared polymer modified g-C_3N_4 nanocomposites (Fig. 10). Obviously, polymer modified g-C_3N_4 nanocomposites shows much decreased arc radius compared with neat g-C_3N_4. The reduced arc radius indicates diminished resistance of working electrodes, suggesting a decrease in the solid state interface layer resistance and the charge transfer resistance across the solid-liquid junction on the surface by forming hybrid structures of g-C_3N_4 with polymer.[29] Since the radius of the arc on the EIS spectra reflects the migration rate occurring at the surface, it suggests that a more effective separation of photogenerated electron-hole pairs and a faster interfacial charge transfer occurs on polymer modified g-C_3N_4 nanocomposites surface under this condition.[30]

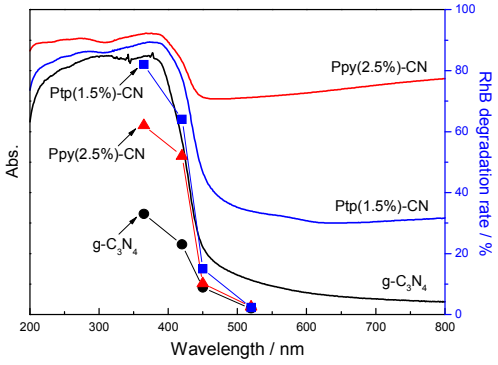

Fig. 11 Wavelength-dependent RhB dagradation rate of g-C_3N_4, Ppy(2.5%)-CN and Ptp(1.5%)-CN.

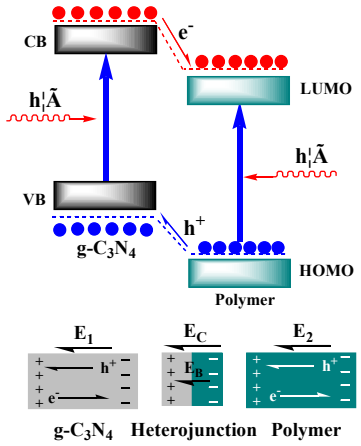

Fig. 12 The schematic illustration of electron-hole separation and transport at the g-C_3N_4/polymer heterojunction interface: E_C is the contact electric field for the two components; E_B is the potential barrier in the interfacial depletion layer; E_1 and E_2 are the internal electric fields induced by the redistribution of the spatial charges in g-C_3N_4 and polymer, respectively.

It was previously reported that the introduction of polymer facilitates the separation and transport of photogenerated carriers, thus enhancing the visible-light photocatalytic activity of g-C_3N_4.[10-13] However, besides this promoting effect, whether polymer with strong visible light absorption acts as visible light sensitizer benefiting the photocatalytic performance is not investigated in previous research. Here, the wavelength-dependent RhB degradation rates of g-C_3N_4, Ppy(2.5%)-CN and Ptp(1.5%)-CN are evaluated (Fig. 11). It is demonstrated that the RhB degradation rates of Ppy(2.5%)-CN and Ptp(1.5%)-CN are obviously higher than that of neat g-C_3N_4 when the light wavelength lower than 450 nm is cutted off. The degradation rate of RhB is in good agreement with the optical absorption. However, when the 520 nm filter is used, the activities of Ppy(2.5%)-CN and Ptp(1.5%)-CN are almost same as neat g-C_3N_4 though their light absorption abilities are much higher than neat g-C_3N_4 (Fig. 11). This means the improved visible light absorption induced by polymer modification does not give rise to enhanced photocatalytic activity of g-C_3N_4 in the visible light region, and hence the modified polymer does not function as visible light sensitizer.

Based on the above conclusion, the possible photocatalytic mechanism is discussed. The HOMO and LUMO levels are +2.67 and -0.18 eV for Ppy and +1.88 and -0.12 eV for Ptp according to previous report.[31] The CB and VB of g-C_3N_4 are -1.12 eV and +1.57 eV, respectively.[3] Therefore, once g-C_3N_4 and polymer are electronically coupled together, the band alignment between the two kinds of materials results in the formation of heterojunction with well-matched band structure. The schematic illustration of electron-hole separation and transport at the g-C_3N_4/polymer heterojunction interface is shown in Fig. 12. Upon visible-light irradiation, the photogenerated electrons tend to transfer rapidly from g-C_3N_4 to Ppy (Ptp) driven by CB offset of 0.94 eV (1.0 eV), whereas the photogenerated holes transfer from Ppy (Ptp) to g-C_3N_4 driven by VB offset of 1.1 eV (0.31 eV). The potential difference is the main driving force for efficient charge separation and transfer. These two charge transfer processes are beneficial for overcoming the high dissociation barrier of the Frenkel exciton and stabilizing electrons and holes. The redistribution of electrons on one side of the heterojunction (polymer) and holes on the opposite side (g-C_3N_4) could establish a steady internal electric fields, which reduces the electron/hole pairs recombination. As the photogenerated electrons and holes are spatially separated into two components, the charge recombination is drastically inhibited, which is of great benefit for enhancing the photocatalytic activity.

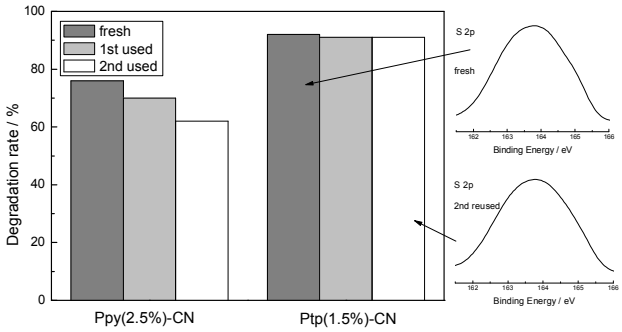

Fig. 13 Photocatalytic stability of Ppy(2.5%)-CN and Ptp(1.5%)-CN.

Fig. 13 shows photocatalytic stabilities of Ppy(2.5%)-CN and Ptp(1.5%)-CN. The photodegradation time is 120 min. No obvious decrease in activity is observed for Ptp(1.5%)-CN after three cycles, indicating good stability of Ptp(1.5%)-CN. However, for Ppy(2.5%)-CN, the activity decreases obviously. This is probably attributed to the different interaction strength between g-C_3N_4 and polymers. Compared with Ppy(2.5%)-CN, the stronger interaction exists between electron-rich g-C_3N_4 and Ptp with strong electronegativity oxygen in C=O bond, leading to a better structural stability of Ptp(1.5%)-CN. No obvious difference is observed in the XPS spectra of fresh and reused Ptp(1.5%)-CN in the region of sulfur (Fig. 13). The sulfur concentrations of fresh and reused Ptp(1.5%)-CN measured by elemental analyse is very close (0.65 wt.% and 0.62 wt.%), which confirms the outstanding structural stability of Ptp(1.5%)-CN. In order to compare the interaction strength between g-C_3N_4 and two polymers, 0.1 g Ppy(2.5%)-CN and Ptp(1.5%)-CN are dispersed in 10 mL water and sonicated for 10 min respectively, and then the suspensions are obtained. For Ptp(1.5%)-CN, the as-prepared nanocomposite in suspension began to sink to the bottom after resting for a while. After 3 min, the solution became clear, indicating that the simultaneous subsiding of g-C_3N_4 and Ptp. This suggests that the Ptp in the solution are completely coupled on the surface of g-C_3N_4 nanoparticles to form a g-C_3N_4/Ptp nanocomposite. However, for Ppy(2.5%)-CN suspensions, partial Ppy roses up to the surface immediately. The formed g-C_3N_4/Ppy nanocomposites sink to the bottom within 2 min. This hints, compared with Ppy, a stronger interaction exists between g-C_3N_4 and Ptp. Compared with fresh Ppy(2.5%)-CN, more Ppy rises up to the surface for reused catalysts. This indicates that the structural damage of nanocomposite occurs,

leading to more g-C_3N_4 and Ppy separation from each other. The deciduous Ppy of fresh and reused Ppy(2.5%)-CN are collected and weighed. The result shows that the loss rate of Ppy is 8 wt.% and 22 wt.% for fresh and reused Ppy(2.5%)-CN. For Ptp(1.5%)-CN, this phenomenon is not observed. Therefore, it is confirmed that the structure of Ptp(1.5%)-CN is more stable than that of Ppy(2.5%)-CN.

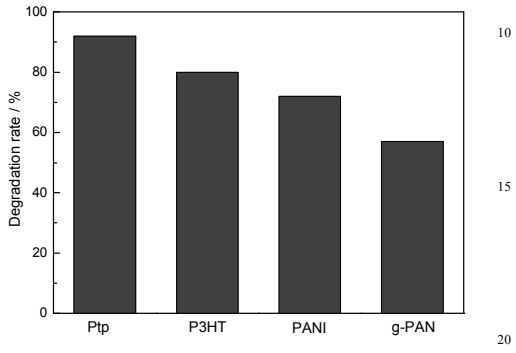

Fig. 14 Photocatalytic performances of Ptp, P3HT, PANI and g-PAN modified g-C_3N_4 in the degradation of RhB under visible light irradiation.

In order to investigate the photocatalytic performance of Ptp(1.5%)-CN, other three polymers, P3HT, PANI and g-PAN, are prepared according to previous reports and used to modify g-C_3N_4 (with the same mass ratio as Ptp(1.5%)-CN) using the same method.[11,13,32] The result shown in Fig. 14 indicates that Ptp modified g-C_3N_4 nanocomposite exhibits the highest photocatalytic activity among those polymers. Thus, it is concluded that Ptp is a optimal polymer to prepare polymer/g-C_3N_4 nanocomposite with excellent photocatalytic activity and stability.

Conclusions

Ppy and Ptp modified g-C_3N_4 nanocomposites are prepared and their photocatalytic performances are compared. The results reveal that no obvious difference is observed in grain size, crystal phase and structural properties between two series of polymer modified g-C_3N_4 nanocomposites. The polymer modification can decrease the band gap which is beneficial for the visible-light absorption. The introduction of polymers does not act as visible light sensitizer but facilitates the separation and transport of photogenerated carriers. The optimal polymer amounts are 1.5 and 2.5 wt.% for Ptp and Ppy modified g-C_3N_4 nanocomposites. The stronger interaction exists between electron-rich g-C_3N_4 and Ptp with strong electronegativity oxygen in C=O bond, leading to a higher electron-hole separation rate and better photocatalytic activity and stability. Among Ptp, P3HT, PANI and g-PAN, Ptp is the optimal polymer to prepare polymer/g-C_3N_4 nanocomposite with excellent photocatalytic activity and stability.

Acknowledgment

This work was supported by Science & Technology Research Foundation of Heilongjiang Province Education Bureau of China (No.12541626), Postdoctoral Fund of Heilongjiang province of China (No. LBH-Z14208), Education Department of Liaoning Province (No. L2014145), Environmental Science and Engineering Innovation Team of Liaoning Shihua University ([2014]-11), and Students' Innovation Fund Project of China.

Notes and references

[a] *College of Chemistry, Chemical Engineering, and Environmental Engineering, Liaoning Shihua University, Fushun 113001, China*
[b] *School of Chemistry and Materials Sciences, Heilongjiang University; Key Laboratory of Chemical Engineering Processes & Technology for High-efficiency Conversion (College of Heilongjiang Province), Harbin 150080, China. E-mail: guangw001@163.com*

1 D.Z. Li, Z.X. Chen and Y.L. Chen, *Environ. Sci. Technol.,* 2008, **42**, 2130.
2 Z.X. Chen, D.Z. Li and W.J. Zhang, *J. Phys. Chem. C.,* 2009, **113**, 4433.
3 X. Wang, K. Maeda and A. Thomas, *Nat. Mater.,* 2009, **8**, 76.
4 K. Sridharan, E. Jang and T.J. Park, *Appl. Catal. B Environ.,* 2013, **142-143**, 718.
5 X.F. Chen, J.S. Zhang and X.Z. Fu, *J. Am. Chem. Soc.,* 2009, **131**, 11658.
6 G. Liu, P. Niu and C.H. Sun, *J. Am. Chem. Soc.,* 2010, **132**, 11642.
7 Y.J. Zhang, T. Mori and J.H. Ye, *J. Am. Chem. Soc.,* 2010, **132**, 6294.
8 Y.J. Zhang, A. Thomas and M. Antonietti, *J. Am. Chem. Soc.,* 2009, **131**, 50.
9 F.Goettmann, A. Fisher and M. Antonietti, *Angew. Chem. Int. Ed.,* 2006, **45**, 4467.
10 L.W. Zhang, H.B. Fu and Y.F. Zhu, *Adv. Funct. Mater.,* 2008, **18**, 2180.
11 H.J. Yan and Y. Huang, *Chem. Commun.,* 2011, **47**, 4168.
12 L. Ge, C.C. Han and J. Liu, *J. Mater. Chem.,* 2012, **22**, 11843.
13 F. He, G. Chen and Y. Yu, *ACS Appl. Mater. Interf.,* 2014, **6**, 7171.
14 H.M. Wang, G.Q. Tang and S.S. Jin, *Acta Chimica Sinic.,* 2007, **65**, 2454.
15 L.N. Geng, S.R. Wang and P. Li, *Chin. J. Inorg. Chem.,* 2005, **21**, 977.
16 F.B. Li, X.Z. Li and M.F. Hou, *Appl. Catal. A Gen.,* 2005, **285**, 181.
17 H.J. Dong, G. Chen, J.X. Sun, C.M. Li, Y.G. Yu and D.H. Chen, *Appl. Catal. B: Environ.,* 2013, **134-135**, 46.
18 J. Lin, Y. Lin and P. Liu, *J. Am. Chem. Soc.,* 2002, **124**, 11514.
19 S.W. Liu, J.G. Yu and M. Jaroniec, *J. Am. Chem. Soc.,* 2010, **132**, 11914.
20 B. Oregan and M. Gratzel, *Nature,* 1991, **353**, 737.
21 G.Q. Li, N. Yang and W.L. Wang, *J. Phys. Chem. C,* 2009, **113**, 14829.
22 F. Dong, Z.W. Zhao, T. Xiong, Z.L. Ni, W.D. Zhang, Y.J. Sun, W.K. Ho, *ACS Appl. Mater. Interfaces,* 2013, **5**, 11392.
23 S.C. Yan, Z.S. Yan and Z.G. Zou, *Langmuir,* 2009, **25**, 10397.
24 Y.S. Qiao, L.Z. Shen and M.X. Wu, *Mater. Lett.,* 2014, **126**, 185.
25 S.Z. Hu, F.Y Li and Z.P. Fan, *Dalton Trans.,* 2015, **44**, 1084.
26 J. Heeg, C. Kramer and M. Wolter, *Appl. Surf. Sci.,* 2001, **180**, 36.
27 S.L Bai, K.W. Zhang and J.H. Sun, *Sensor Actuat B.,* 2014, **197**, 142.
28 H. Nakajama, T. Mori and Q. Shen, *Chem. Phys. Lett.,* 2005, **409**, 81.
29 B.L. He, B. Dong and H.L. Li, *Electrochem. Commun.,* 2007, **9**, 425.
30 Q.W. Huang, S.Q. Tian and D.W. Zeng, *ACS Catal.,* 2013, **3**, 1477.
31 U. Salzner, J.B. Lagowski, P.G. Pickup, R.A. Poirier, *Synthetic Metals,*1998, **96**, 177.
32 X.F. Wang, Y.H. Shen, A.J. Xie, L.G. Qiu, S.K. Li and Y. Wang, *J. Mater. Chem.,* 2011, **21**, 9641.

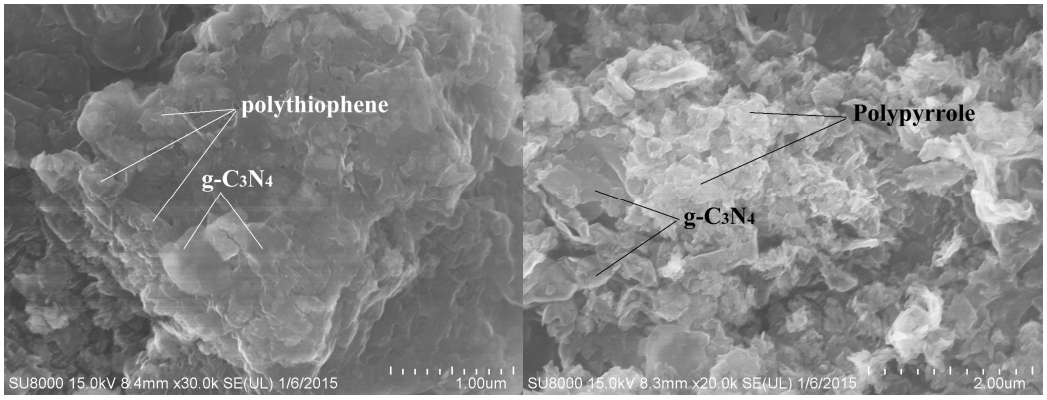

Polythiophene modified g-C_3N_4 exhibits stronger interaction with g-C_3N_4 and higher electron-hole separation rate than that of polypyrrole, thus shows a better photocatalytic activity and stability.